INTERNATIONAL SOCIETY FOR SOIL MECHANICS AND GEOTECHNICAL ENGINEERING

Effect of land cover and climate changes on rainfall-induced landslides. Regional-scale modelling in the Val d'Aran (Pyrenees, Spain).

M. Hürlimann, V. Medina, A. Lloret, J. Vaunat, C. Puig-Polo, J. Moya

Department of Civil and Environmental Engineering, BarcelonaTECH UPC, Spain

marcel.hurlimann@upc.edu

Abstract

The analysis of the impacts of future environmental changes on rainfall-induced landslides is of great importance. Recent studies have shown that these changes will affect the frequency and magnitude of shallow slides and debris flows. In this study, we focused on the effects of climate changes as well as land use and land cover (LULC) changes on rainfall-induced slope failures at regional scale. A newly developed physically-based susceptibility model was applied and the Val d'Aran area, located in the Central Pyrenees (Spain), was selected as study site.

First, the catastrophic landslide episode, which affected the Val d'Aran area in June 2013, was used for a preliminary validation of the susceptibility model. Then, the future LULC changes until the end of the 21th century were simulated in the study area and incorporated in the regional landslide model. The results revealed an overall increase of stability in the future, because of the larger area of forest and the consequent higher cohesion due to augmented root strength. In the next step, the impacts of future climate changes were calculated including a higher rainfall intensity. We assumed an increase of 15%, which corresponds to the last findings obtained from the ensemble of regional climate models using RCP 4.5 and 8.5 scenarios. This increase in rainfall intensity produced a reduction of the overall slope stability in the study area. However, comparing the effects produced by LULC and rainfall changes revealed that the LULC changes have a greater influence than the changes related to the rainfall conditions. This means that the overall stability in the study area slightly improves in the future.

Multiples assumptions and simplifications were introduced in these preliminary calculations of the future landslide susceptibility, and additional simulations are necessary to confirm the observed trends. Nevertheless, the results seem to be coherent with the outcomes of other recent studies and give some valuable information for both stakeholders and researchers, which deal with the same thematic.

1 INTRODUCTION

Rainfall-triggered landslides are an important hazard in mountainous regions. In the Pyrenees, such mass movements may not occur as frequent as in other mountain ranges, but they represent a considerable hazard not only regarding land degradation and sediment yield, but also concerning damages at infrastructures and buildings.

Recent studies concluded that land use and land cover (LULC) and climate changes will have an important effect on the frequency and magnitude of rainfall-induced landslides (Bernardie et al., 2017; Gariano and Guzzetti, 2016; Persichillo et al., 2017; Shu et al., 2019). Some investigations applied physical-based stability models to analyze the impacts of future changes on the spatial and temporal probability of landslides at regional scale (Vanacker et al. 2003; Van Beek and Van Asch 2004; Alvioli et al. 2018). However, the assessment of the effects of LULC and climate changes on shallow slides and debris flows is complex and uncertainties are still very large.

In this study, we present preliminary results of the assessment of landslide susceptibility at regional scale applying a newly developed physical-based model with a stochastic approach. The model is applied to the Val d'Aran study area (Pyrenees, Spain), where also the impacts of future changes (LULC and climate) are determined.

The goals of this publication are manifold: i) the presentation of a new regional-scale physically-based landslide susceptibility model, ii) the evaluation of the impacts of future LULC changes in the Val d'Aran area, iii) the analysis of the effects of climate changes, and iv) the assessment of the impacts of the combined effects including LULC and climate changes.

2 SETTINGS

2.1 Val d'Aran study area

The Val d'Aran study area is located in the Central Pyrenees and covers 336 km^2. The capital is Vielha and the entire administrative region has a population of about 10000 persons.

The morphology of the study region is a typical high-mountain area ranging from about 1000 m asl at the valley floor, where the Garonne River drains to France, up to the surroundings peaks of 2750 m asl. Fluvial and glacial processes strongly affected the landscape and formed many steep slopes that are susceptible for different types of slope mass-wasting.

From a geological point of view, the Val d'Aran area is located in the Axial Pyrenees (Muñoz, 1992). The bedrock mostly consists of folded Paleozoic rocks, Mesozoic and Tertiary sediments and tardohercinian plutonic intrusions. The superficial formations principally include colluvium and glacial deposits.

The average annual precipitation oscillates between about 900 mm in the valley floor (~1000 mm in Vielha) and ~1200 mm in the higher part of the study area. The average annual temperature is ranging from 5 to 9 degrees Celsius.
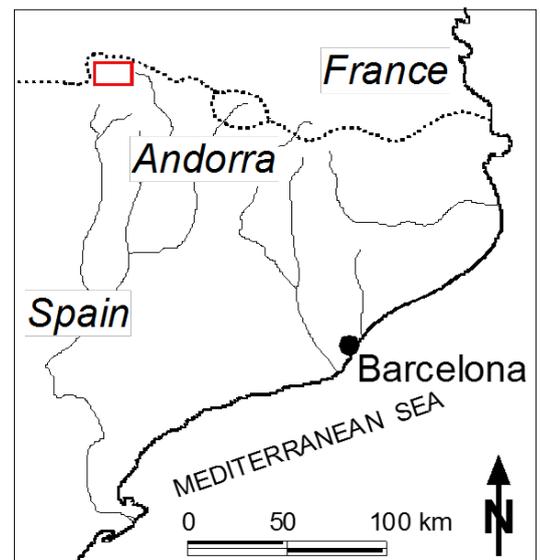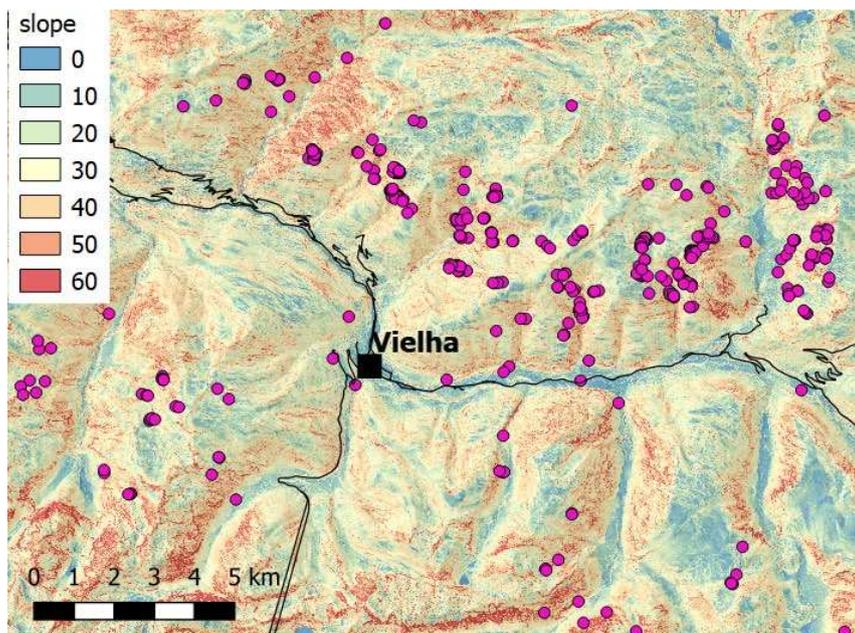

Figure 1. Left: The Val d'Aran study area. Background is a slope angle map with a shaded relief. The dots indicate the landslide initiation points of the 2013 episode. Right: Overview map indicating the location of the study area by the red rectangle.

2.2 The 2013 landslide episode

An exceptional flood and landslide episode occurred on June 17 and 18, 2013 in the Val d'Aran area (Victoriano et al., 2016; Shu et al., 2019). Hundreds of shallow slides and debris flows were triggered by the combination of important snowmelt and very high rainfall.

A landslide inventory of 393 initiation points was created after the episode by interpretation of aerial photographs, helicopter flights and field surveys.

The analysis of the initiation points revealed that LULC played an important role and density of slope failures was much higher in scree and grassland than in forested areas. See Shu et al. (2019) for more information on the governing factors of the landslides and debris flows.

3 METHODS

3.1 Land use and land cover modelling

Herein, the land use and land cover (LULC) was simplified and finally reclassified into six types: forest, shrubs, grassland, scree, water bodies, urban areas. The extensions of these six LULC types were delineated from aerial photograph of 1990 and 2013 and the resulting maps were used as input data for the future evolution. In this study, the prediction of LULC maps for 2049 and 2097 were calculated by the Land Change Modeler software of the IDRISI TerrSet software suite (Eastman, 2015). The predictor variables incorporated into the LULC modelling are divided into three categories: climatic, topographic and landscape variables. Detailed explanation on the modelling and the resulting maps can be found in Shu et al. (2019).

3.2 Climate change modelling

The climate change is introduced in the landslide calculations using the Climate Change Factor (*CCF*, Arnbjerg-Nielsen, K., 2008, Rodriguez et al., 2014). For our study area, the values were taken from the RESCCUE EU Project (http://www.resccue.eu), where the intensity-duration-frequency curves (IDF curves) were calculated for the climate change prediction in Barcelona (Monjo et al., 2018). The *CCF* is computed combining the ensemble of 10 models results (using data from CMIP5) and selecting the RCP 4.5 and 8.5 scenarios. In the RESSCCUE-project, it was concluded that the expected *CCF* for the end of the 21st century may be between 1.1 and 1.2. Therefore, a final value of *CCF* equal to 1.15 was selected in our stability calculations of the Val d'Aran.

3.3 Regional stability model FSLAM

3.3.1 Methods

In the following, we present a newly developed model that calculates the susceptibility of shallow slope failures at regional scale (herein called "FSLAM"). As in many other models, we applied the common infinite slope approach (Lambe and Whitman 1991), which determines the Factor of Safety (*FS*) in each cell of the input raster by

$$FS = \frac{C}{\gamma_s z \cos \theta \sin \theta} + \left(1 - \left(\frac{h}{z}\right)\left(\frac{\gamma_w}{\gamma_s}\right)\right)\left(\frac{\tan \varphi}{\tan \theta}\right) \quad (1)$$

, where C is the cohesion, γ_s the saturated soil unit weight, γ_w the water unit weight, θ is the terrain slope, ϕ the internal friction angle, h the water table depth and z the soil depth. Both h and z are measured in the vertical direction. In this study, the cohesion is defined as

$$C = C_s + C_r \quad (2)$$

, where C_s is the effective cohesion related to the soil matrix and C_r is the apparent cohesion produced by the root strength.

Regarding the pore-water pressure or the value of h, the FSLAM-model merges two different approaches and two separate time scales. The antecedent rainfall is calculated by the "lateral flow" theory, which determines the pore-water pressure in each cell by its contributing drainage area (Montgomery and Dietrich, 1994; Pack et al., 1998). In contrast, the event rainfall is calculated by the "vertical flow" or vertical infiltration of rainfall in each cell (Baum et al., 2010; Iverson, 2000). When incorporating these two approaches that finally computes the value of h in each cell, the initial equation of *FS* (Eq. 1) can be transformed into

$$FS = \frac{C}{\gamma_s z \cos \theta \sin \theta} +$$
$$\left(1 - \left(\left(\frac{a}{b}\right)\frac{q_a}{K_h z \sin \theta \cos \theta} + \frac{q_e}{n \cdot z}\right)\left(\frac{\gamma_w}{\gamma_s}\right)\right)\left(\frac{\tan \varphi}{\tan \theta}\right) \quad (3)$$

, where a is the drainage area, b the cell size, K_h the horizontal hydraulic conductivity, q_a the average infiltration rate due to antecedent rainfall, q_e the storm event infiltration, and n the porosity.

On one side, the antecedent rainfall infiltration, q_a, is directly defined by precipitation intensity units (e.g., mm/h or mm/d). Therefore, the value of q_a can be determined by averaging the total precipitation in a time window and taking into account the effect of evapotranspiration. The user must decide the length of the window depending on the hydrogeological properties and the rainfall conditions.

On the other side, the event infiltration, q_e, is computed combining the event precipitation and the soil runoff. In order to obtain the q_e-value, a simple, but well-known method in hydrology is applied: the runoff curve number or SCS-CN method (USDA, 1986). In this method, the relation between precipitation-runoff-infiltration only depends on one single parameter, which is the curve number (CN). CN is an empirical parameter that can determined by the soil type and vegetation cover.

In conclusion, the FSLAM-model depends on seven soil parameters (C_s, C_r, ϕ, K_h, γ_s, n, z), one related to the rainfall-runoff-infiltration relationship (CN), two morphologic variables (a/b, θ) and two precipitation variables (q_a, q_e). The soil parameters may be assumed to have a stochastic distribution, which can be defined by a probability density function. However, due to the complexity of the stochastic equation, it is not possible to obtain an analytical solution for all the possible probability density functions. Hence, a numerical integration is necessary to solve the stochastic safety factor equation. In this work, we finally decided that only the internal friction angle ϕ and the cohesion C are assumed to be normally distributed. This permits using the theory developed by Simoni et al. (2008), where an analytical solution is developed for the stochastic factor of safety equation. The selection of ϕ and C as stochastic variables is justified by their importance in Eq. (3), which was observed during the sensitivity analysis that was performed (for details see: Medina et al., accepted).

The final output of the FSLAM-model is the probability of failure, PoF, which is calculated in each cell of the study area. PoF is defined as the probability of $FS < 1$ assuming the probability density function of internal friction angle and cohesion.

3.3.2 Input data

First, there are the two morphometric variables that are calculated in each cell from the Digital Elevation Model (DEM). In this study, a DEM with a 5 m cell size was obtained from the Cartographic and Geological Institute of Catalonia (www.icgc.cat). The FSLAM-model directly calculates the slope and the upstream drainage area of each cell.

Second, the hydrological and geotechnical properties of the different soil types have to be determined. Generally, there are no detailed field data and the properties have to be derived from available maps that include information on lithology. However, the correlation between lithological units and soil characteristics in not always straightforward and includes many uncertainties (e.g. Tofani et al. 2017). In this preliminary study, several assumptions and simplifications were made to overcome this problem. First of all, soil unit weight, porosity and hydraulic

conductivity were assumed to be constant in the entire study area using the following values: $\gamma_s = 20$ kN/m^3, $n = 0.25$ and $K_h = 5.18$ m/day (e.g. www.geotechdata.info/parameter). In addition, the soil matrix is assumed to be cohesionless ($C_s = 0$ kPa) and therefore, only the root strength, C_r, affects the total cohesion (thus, $C = C_r$). The assumption of cero soil matrix cohesion may not represent the real situation, but was selected in this preliminary work due to the lack of geotechnical data in the study area and because the goal of this study was to analyze the influence of LULC-changes.

Finally, the existing LULC map (CREAF 2009) was used to determine the three remaining soil parameters: the root strength, C_r, friction angle, ϕ and soil thickness, z. The original LULC map was simplified into six classes and the values of the three soil parameters are listed in Table 1. As previously described, C_r and ϕ are introduced in the FSLAM-model using a normal distribution. Thus, they are given by minimum and maximum values. The assumption to link soil properties with LULC is an important simplification, but it has the great advantage that it permits the detailed analysis of the effect of LULC-changes, which is one of the major goals of this study.

Table 1. Value of apparent root cohesion, friction angle and soil thickness of the four principal LULC classes used in this study.

LULC	Cr_{min} (kPa)	Cr_{max} (kPa)	ϕ_{min} (º)	ϕ_{max} (º)	z (m)
forest	5	20	20	35	1.35
shrubs	1	15	20	35	1.4
grass	0.5	10	20	35	1.45
scree-rock	0	0	30	45	1.45

As another input, the curve number is needed as a spatially distributed raster input for the entire study area. This information is defined in the technical report on the calculation of the maximum discharge in rivers (CEDEX, 2011) and can be downloaded from the website of the Spanish Ministry (www.miteco.gob.es/va/cartografia-y-sig/). Finally, the water unit weight was assumed to be $\gamma_w = 9.81$ kN/m^3.

Third, the two precipitation variables have to be defined. We assumed that both variables are constant over the entire study area; not only for the 2013 rainfall episode, but also for the future predictions. For the validation of the model, we used the 2013 landslide episode, which was caused by a combination of important snowmelt previous to the episode and a high rainfall amount that finally triggered the slope failures. The snowmelt was incorporated into the model by the antecedent rainfall

value with a water equivalent of 1 mm/day in order to calculate the initial degree of saturation of the superficial soil layers. Then, the triggering rainfall was assumed to be 100 mm. As stated above, both antecedent and triggering rainfalls were applied homogenously over the entire study area. These are very simplified conditions, but represent rather well the climatic situation that finally triggered the slope failures in the study area.

4 RESULTS

4.1 Validation of stability model

The probability of failure of the 393 initiation points was computed using on one side the LULC map of 2013, the 5m DEM and the CN-map. On the other side, the simplified conditions of the snowmelt

as well as rainfall and the soil properties described in the previous section, were incorporated.

The resulting map that indicates the probability of failure in each grid cell of the study area is shown in Figure 2a. Since the rainfall conditions are homogeneous over the entire study area, the probability of failure in each cell mainly depends on the slope angle and LULC class, while the drainage area plays a minor role. Therefore, the effect of root cohesion is important and the different LULC are clearly visible. This can be observed by the lower failure probability at the south-facing slopes of the main valley (between Vielha and Salardú), in contrast to the more stable conditions at the north-facing slopes. This difference is due to the fact that south-facing slopes are principally covered by grass and shrubs, whereas forest grows at the north-facing slopes.
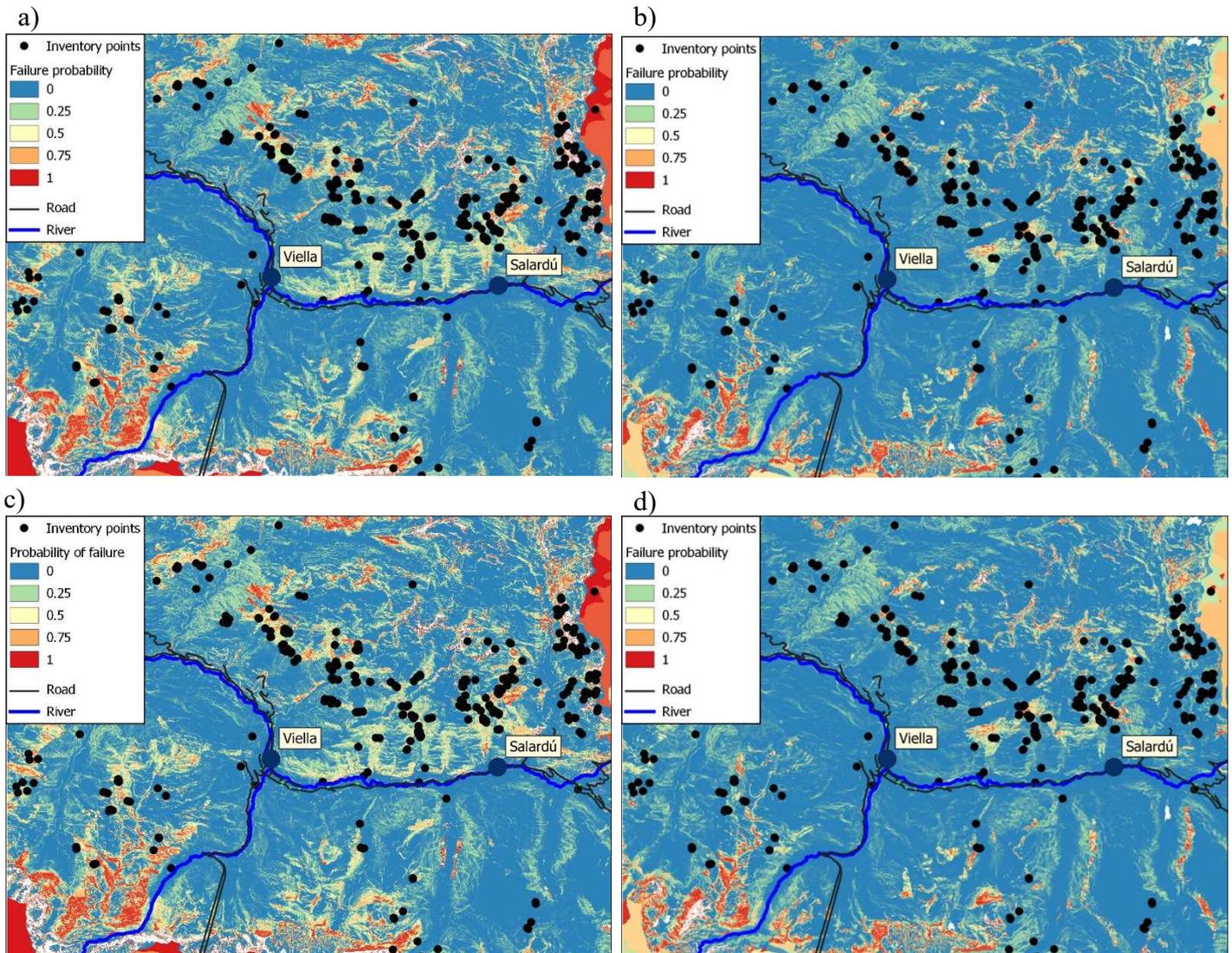

Figure 2. Computed landslide susceptibility of the Val d'Aran study area for present and future conditions. a) Probability of failure in each cell for the 2013 landslide episode. b) Prediction of future changes including the LULC conditions of 2097. c) Prediction of future changes incorporating the future rainfall conditions of 2100. d) Prediction of future changes including both future changes.
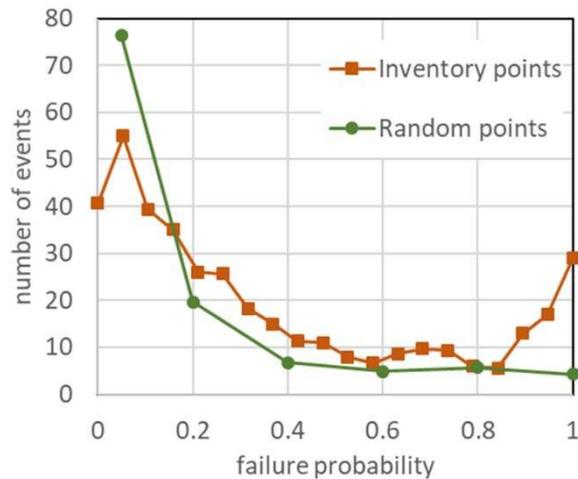
Figure 3. Validation of the FSLAM-model comparing the 393 initiation points of the 2013 landslide episode with 393 randomly selected points.
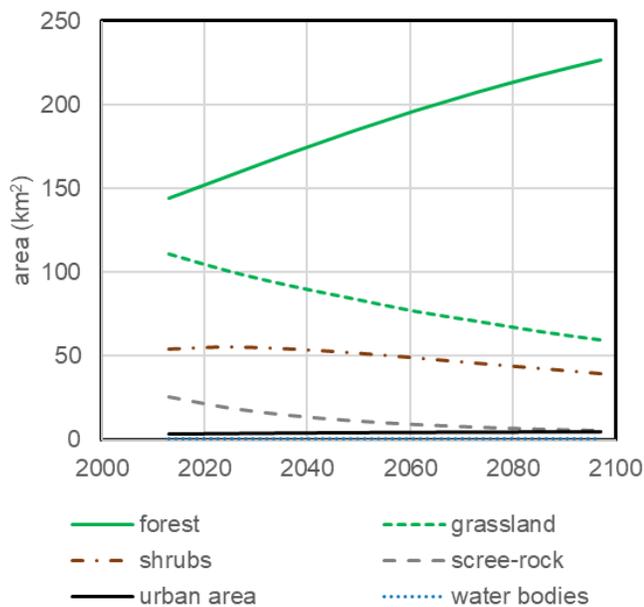

Figure 4. LULC prediction in the study area until 2097 (adapted from Shu et al. 2019).

The failure probability of the 393 initiation points, which are included in the 2013 inventory, were compared to the one of 393 randomly selected grid cells, which are representing points with stable conditions (Figure 3). The two curves allows a preliminary evaluation of the performance of the FSLAM-model. The results show that there are generally more inventory points in the range of higher failure probability (preferably instable conditions), while there is a clear larger amount of random points comparing stable conditions (failure probability less than 0.2).

This validation process can definitively be improved, but the results are acceptable for a preliminary analysis. In addition, the goal of this study is to analyze the effects the future changes by a physically-based model and the back analysis of the 2013 landslide episode confirmed that the FSLAM-model is producing consistent stability conditions.

4.2 Effect of future changes

In a first step, the LULC predictions and their impacts on the landslide susceptibility were investigated. The LULC modelling showed that historic trends are mostly continuing in the future (simulation until 2097), which means that forest areas will increase, while grassland and meadows will decrease (Shu et al. 2019; Fig. 4).

When these future LULC-changes were included in the FSLAM-model, the results revealed an overall increase of stability (Fig. 2b). This can be explained by the larger area of forest and the resulting higher cohesion due to the root strength in these areas. The increase of stability may be better visualized by the cumulative distribution function, *CDF,* and comparing the results obtained for the LULC-changes with the ones of the conditions of 2013. The *CDF* curves include the failure probability of all the pixels in the study area (Fig. 5). In order to compare the two resulting curves in a quantitative way, the area under the curve, *AUC*, is calculated for each *CDF*. The *AUC* of the present (2013) conditions is 0.891, while the *AUC* obtained for LULC changes is 0.899. This confirms the overall increase of stability that was already visible comparing the two susceptibility maps of Fig. 2.

In the next step, the effects of climate changes on the landslide susceptibility were analyzed. In the simulation, the antecedent rainfall was maintained as 1 mm/day, but the event rainfall was increased 15 % as explained previously. Therefore, the event or triggering rainfall was assumed to be 115 mm. The resulting susceptibility map shows a slight overall decrease of stability and the increase of failure probability is mostly rather small (Fig. 2c). The *CDF* curve is given in Fig. 5 and the corresponding *AUC* is 0.881; slightly lower than the one for the present conditions, which is 0.891.
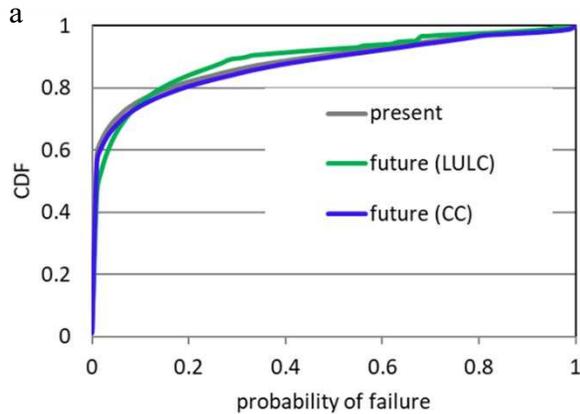
a

Figure 5. Effect of future changes on the landslide susceptibility. Representation of the different cumulative distribution function (CDF) curves. The present (year 2013) conditions are compared with the ones of land use and land cover (LULC) of 2097 and rainfall conditions (CC) of 2100.

Finally, the cumulative effects of the two changes (LULC and climate changes) are included in the modelling and the susceptibility map was calculated. The results show that there is a slight overall increase of stability (Fig. 2d). As previously stated, the positive and stabilizing influence of the LULC changes exceed the destabilizing effects related to the climate changes. The AUC of the CDF curve, which includes the two environmental changes, is 0.897 in comparison with the AUC of the present conditions, which is 0.891).

5 CONCLUSIONS

In this study, the effects of climate and land cover changes on rainfall-induced shallow slides were investigated applying a regional physically-based susceptibility model. The results of the preliminary susceptibility assessment exposed several important aspects.

On one side, the overall stability increases in the study area, when we include the future LULC changes in the calculations. This is basically related to the augment of forest cover and the subsequent higher root strength in these areas.

On the other side, the predictions of future rainfall conditions produce a decrease of the overall stability in the study area, because the intensity of the triggering rainfall is higher.

An important outcome was revealed, when the impacts of both changes were compared. This comparison exposed that the LULC changes have a higher influence than the changes associated with the rainfall conditions. Therefore, the overall stability conditions will improve in the future considering both the climate and the land cover changes in the susceptibility mapping.

Multiples assumptions and simplifications were introduced in these preliminary calculations, but the outcomes seem to be coherent and reveal the general effects related to the impacts of future changes of land cover and rainfall conditions.

The present study was carried out in Val d'Aran, a high-mountain valley located in the Central Pyrenees. However, we believe that the future trends obtained in this study may be similar in other mountainous areas, where climate and vegetation is similar regarding present conditions and future predictions.

6 ACKNOWLEDGEMENTS

7 REFERENCES

Alvioli, M., Melillo, M., Guzzetti, F., Rossi, M., Palazzi, E., von Hardenberg, J., Brunetti, M.T., Peruccacci, S. (2018). "*Implications of climate change on landslide hazard in Central Italy.*" Sci. Total Environ. 630, 1528–1543.

Arnbjerg-Nielsen, K., (2008). "*Quantification of climate change impacts on extreme precipitation used for design of sewer systems*". In Proceedings of the 11th international conference on urban drainage (vol. CD-ROM).

Baum, R.L., Godt, J.W., Savage, W.Z., (2010). "*Estimating the timing and location of shallow rainfall-induced landslides using a model for transient, unsaturated infiltration*". J. Geophys. Res. Earth Surf. 115. doi.org/10.1029/2009JF001321

Bernardie, S., Vandromme, R., Mariotti, A., Houet, T., Grémont, M., Grandjean, G., Bouroullec, I., Thiery, Y., (2017). "*Estimation of Landslides Activities Evolution Due to Land--Use and Climate Change in a Pyrenean Valley*", in: Mikos, M., Tiwari, B., Yin, Y.,

Sassa, K. (Eds.), Advancing Culture of Living with Landslides: Volume 2 Advances in Landslide Science. Springer International Publishing, Cham, pp. 859–867.

CEDEX (2011). "*Mapa de caudales máximos. Memoria técnica*". Madrid: Centro de Estudios Hidrográficos del CEDEX. 73pp.

CREAF (2009) "*Soil cover map of Catalonia (MSC-4)*". https://www.creaf.uab.es/mcsc/.

Eastman, J.R., (2015). "*TerrSet: Geospatial Monitoring and Modeling Software*". Clark Labs 53.

Gariano, S.L., Guzzetti, F., (2016). "*Landslides in a changing climate*". Earth-Science Rev. 162, 227–252.

Iverson, R.M., (2000). "*Landslide triggering by rain infiltration*". Water Resour. Res. 36, 1897–1910.

Lambe, T.W., Whitman, R. V, (1979). "*Soil mechanics*". Wiley, New York. 553pp.

Medina, V., Hürlimann, M., Guo, Z., Lloret, A., Vaunat, J. (accepted). "*Fast physically-based model for rainfall-induced landslide susceptibility assessment at regional scale*". CATENA.

Monjo, R., Paradinas, C., Gaitán, E., Redolat, Dario, P. C., Pórtoles, J., Ribalaygua, J. (2018). "*Report on extreme events prediction*". D1.3. RESCCUE Project.

Montgomery, D.R., Dietrich, W.E., (1994). "*A physically based model for the topographic control on shallow landsliding*". Water Resour. Res. 30, 1153–1171.

Muñoz, A., (1992). "*Evolution of a continental collision belt: ECORS-Pyrenees crustal balanced cross-section*", in: McClay, K.R. (Ed.), Thrust Tectonics. Chapman & Hall, pp. 235–246.

Pack, R.T., Tarboton, D.G., Goodwin, C.N., (1998). "*The SINMAP approach to terrain stability mapping*". 8th Int. Congr. Int. Assoc. Eng. Geol. Environ. Proceedings, Vols 1-5 1157–1165.

Persichillo, M.G., Bordoni, M., Meisina, C., (2017). "*The role of land use changes in the distribution of shallow landslides*". Sci. Total Environ. 574, 924–937.

Rodríguez, R., Navarro, X., Casas, M.C., Ribalaygua, J., Russo, B., Pouget, L. and Redaño, A., (2014). "*Influence of climate change on IDF curves for the metropolitan area of Barcelona (Spain)*". International Journal of Climatology, 34(3), pp.643-654.

Shu, H., Hürlimann, M., Molowny-Horas, R., González, M., Pinyol, J., Abancó, C., Ma, J., (2019). "*Relation between land cover and landslide susceptibility in Val d'Aran, Pyrenees (Spain): Historical aspects, present situation and forward prediction*". Sci. Total Environ. 693, 133557.

Simoni, S., Zanotti, F., Bertoldi, G., Rigon, R., (2008). "*Modelling the probability of occurrence of shallow landslides and channelized debris flows using GEOtop-FS*". Hydrol. Process. 545, 532–545.

Tofani, V., Bicocchi, G., Rossi, G., Segoni, S., D'Ambrosio, M., Casagli, N., Catani, F., (2017). "*Soil characterization for shallow landslides modeling: a case study in the Northern Apennines (Central Italy)*". Landslides 14, 755–770.

USDA (1986). "*Urban hydrology for small watersheds. Technical Release 55*". United States Department of Agriculture. Natural Resources Conservation Service, Conservation Engineering Division. 164pp.

Van Beek, L.P.H., Van Asch, T.W., (2004). "*Regional Assessment of the Effects of Land-Use Change on Landslide Hazard By Means of Physically Based Modelling*". Nat. Hazards 31, 289–304.

Victoriano, A., García-Silvestre, M., Furdada, G., Bordonau, J., (2016). "*Long-term entrenchment and consequences for present flood hazard in the Garona River (Val d'Aran, Central Pyrenees, Spain)*". Nat. Hazards Earth Syst. Sci. 16, 2055–2070.